

Rotating Quark Star in Chiral Colour Dielectric Model

Abhijit Bhattacharyya^{a*} and Sanjay K. Ghosh^{b†}

^a *Department of Physics, Scottish Church College, 1 & 3, Urquhart Square, Kolkata - 700 006, INDIA*

^b *Department of Physics, Bose Institute, 93/1, A.P.C. Road, Kolkata - 700 009, INDIA*

The properties of rotating quark star is studied using the equation of state obtained from Chiral Colour Dielectric model. The results are compared with the MIT bag model results. The frequencies in the corotating innermost circular orbits for different central densities are evaluated and compared with the observational results.

PACS number(s):26.60.+c

I. INTRODUCTION

The quark structure of hadrons suggests the possibility of a phase transition from nuclear to quark matter at high density. Since the inception of the concept of phase transition to strange quark matter (SQM) at high density and the possibility of the existence of exotic compact objects [1], several calculations have been done to investigate the existence of quark stars [2] or quark core in neutron stars using different models [3]. The phase transition to strange quark matter has been shown [4] to result in the production of large amount of energy along with the neutrinos. But an unambiguous identification of such processes, for example, in the form of gamma-ray bursters has not been possible till date. On the other hand, Glendenning *et al.* [5] have argued that anomalous behaviour of braking index may be a signature of phase transition to quark matter. Subsequently, studies of braking index using different models [6,7] has been reported. Twin star solutions has also been obtained for both static as well as rotating stars [7] - [9].

At present, despite various studies, there is no consensus regarding the existence of quark stars in the universe. Most of the calculations on the static properties of quark star do not yield any significant observable to distinguish them from neutron stars.

The study of exotic compact objects, like quark stars, has once again become important in the context of compact X-ray and γ -ray sources [10]. Several studies on rotating compact objects have reported a substantial difference in the properties of rotating strange quark and neutron star, attributed mainly to their different equation of state [11,13]. In particular, qualitative differences in the properties of the innermost stable circular orbits (ISCO) of strange quark stars and neutron stars have been found [12,13]. Moreover neutron star calculations yield lower values for ISCO frequencies compared to the quark stars [14]. It has been shown that a comparison of the theoretical value obtained for the ISCO with the kHz quasi periodic oscillations (QPO) found in low mass X-ray binaries (LMXB) can be used to constrain the SQM models.

In the present paper we have studied the rotating strange quark star in the general relativistic framework using the nonlinear Chiral extension of Colour Dielectric Model. The Chiral Colour Dielectric model (CCDM) has been used earlier to study baryon spectroscopy [15] as well as the static properties of nucleons in nuclear medium [16]. These calculations have shown that the model is able to explain the static properties of light baryons very well. Furthermore, when applied to the quark matter calculation, the model yields an equation of state which is quite similar to the one obtained from lattice calculations for zero baryon chemical potential [17]. It has also been used for the calculation of the properties of dibaryons [18], static hybrid stars (neutron stars with quark core) [19] and static strange quark

*E-Mail :bhattacharyyaabhijit_10@yahoo.co.uk

†E-Mail : sanjay@bosemain.boseinst.ac.in

stars [20]. The CCDDM differs from the bag model in several aspects. First of all, in the CCDDM, the confinement of quarks and gluons is achieved dynamically through the colour-dielectric field. In the bag model this is done by hand. Also the quark masses used in the CCDDM are different from those used in the bag model. In the bag model, u and d masses are taken to be zero. The CCDDM requires that these masses are nonzero. It has been found [15] that to fit baryon masses, the required u and d masses are $\sim 100MeV$. Thus, the values of quark masses in CCDDM are closer to the constituent quark masses. Motivated by the earlier successes of the CCDDM we have used this model for the study of rotating quark star.

The paper is organized as follows. In the section 2 a brief description of the CCDDM is presented. Calculations for the rotating star is described in section 3 followed by a summary in the last section.

II. CHIRAL COLOUR DIELECTRIC MODEL

The Lagrangian density of CCDDM is given by [17]

$$\begin{aligned} \mathcal{L}(x) = & \bar{\psi}(x) \{ i\gamma^\mu \partial_\mu - (m_0 + m/\chi(x)U_5) + (1/2)g\gamma_\mu \lambda_a A_\mu^a(x) \} \psi \\ & + f_\pi^2/4Tr(\partial_\mu U \partial^\mu U^\dagger) - 1/2m_\phi^2\phi^2(x) - (1/4)\chi^4(x)(F_{\mu\nu}^a(x))^2 \\ & + (1/2)\sigma_v^2(\partial_\mu \chi(x))^2 - U(\chi) \end{aligned} \quad (1)$$

where $U = e^{i\lambda_a \phi^a/f_\pi}$ and $U_5 = e^{i\lambda_a \phi^a \gamma_5/f_\pi}$, $\psi(x)$, $A_\mu(x)$, and $\chi(x)$ and $\phi(x)$ are quark, gluon, scalar (colour dielectric)and meson fields respectively. The quark and meson masses are denoted by m and m_ϕ respectively, f_π is the pion decay constant, $F_{\mu\nu}(x)$ is the usual colour electromagnetic field tensor, g is the colour coupling constant and λ_a are the Gell-Mann matrices. The flavour symmetry breaking is incorporated in the Lagrangian through the quark mass term $(m_0 + m/\chi U_5)$, where $m_0 = 0$ for u and d quarks. So masses of u, d and s quarks are m , m and $m_0 + m$ respectively. So for a system with broken flavour symmetry, strange quark mass will be different from u and d quark masses. The meson matrix then consists of a singlet η , triplet of π and quadruplet of K . With $m_0 = 0$, one can recover a symmetric three flavour quark matter system. The corresponding meson matrix Φ then becomes a eight component field.

The self interaction $U(\chi)$ of the scalar field is assumed to be of the form

$$U(\chi) = \alpha B \chi^2(x) [1 - 2(1 - 2/\alpha)\chi(x) + (1 - 3/\alpha)\chi^2(x)] \quad (2)$$

so that $U(\chi)$ has an absolute minimum at $\chi = 0$ and a secondary minimum at $\chi = 1$. The interaction of the scalar field with quark and gluon fields is such that quarks and gluons can not exist in the region where $\chi = 0$. In the limit of vanishing meson mass, the Lagrangian of eqn.(1) is invariant under chiral transformations of quark and meson fields.

In general there are approaches which can be followed in the studies of hadronic systems using chiral models. One is the perturbative methodology of cloudy bag model [21]. The another one is hedgehog approach [22], which is nonperturbative but is not applicable for infinite matter. A different ansatz has been proposed in ref. [17] in an attempt to go beyond the perturbative approach of cloudy bag model, One can assume that because of nonvanishing quark and antiquark densities, the square of the expectation value of meson fields develop a nonzero value i.e. $\langle \phi^2 \rangle \neq 0$. On the other hand it is assumed that the expectation value of the meson field vanishes in the medium . For an infinite system of quarks one can take $\langle \phi^2 \rangle$ to be independent of space and time. The meson excitations are then defined in terms of the fluctuations about $\langle \phi^2 \rangle$, so that $\phi^2 = \langle \phi^2 \rangle + \phi'^2$. Defining $F_\phi = \langle \phi^2 \rangle / f_\pi^2$, the CCDDM Lagrangian can be rewritten in terms of F_ϕ s and meson excitations ϕ' [17]. The scalar field χ and F_ϕ have been calculated in the mean field approximation and quark- gluon, gluon- gluon and quark- meson excitations are treated perturbatively.

With the above ansatz, the quark masses now become density dependent through F_ϕ . It has been shown earlier [17] that for three flavour matter only $\langle \vec{\pi}^2 \rangle$ develops non zero value and $\langle K^2 \rangle = \langle \eta^2 \rangle = 0$ which means that strange quark mass remains constant in the medium. The u and d quark masses decrease in the medium with

increase in density. The chemical equilibrium and charge neutrality among the constituents implies $\mu_{d(s)} = \mu_u + \mu_e$ and $(2/3)n_u - (1/3)n_d - (1/3)n_s - n_e = 0$ respectively. Baryon density $n_B = (1/3)\sum_i(n_i)$ where $i = u, d, s$. With these conditions we calculate the thermodynamic potential up to second order in quark-gluon interaction. The parameter set used in the present paper are $B^{1/4} = 152$ MeV, $m_{u,d} = 92$ MeV, $m_s = 295$ MeV, $\alpha = 36$ MeV and strong coupling constant $g_s (= 4\pi\alpha_s) = 1.008$.

III. ROTATING STAR SOLUTIONS

In this section we are going to have a brief discussion of the procedure of the rotating star calculations followed by the discussion of our results obtained. In figure 1 we have plotted the EOS for CCDM along with the bag model results for interacting quark matter with the same bag pressure and strong coupling constant as given for CCDM. The EOS for CCDM is found to be soft compared to that for the bag model.

Once the EOS is obtained the next job is to solve the Einstein's equations for the rotating stars using the EOS. To solve the Einstein's equations we follow the procedure adopted by Komatsu *et.al.* [23]. In this work we briefly outline some of the steps only. The metric for a stationarily rotating star can be written as [24]

$$ds^2 = -e^{\gamma+\rho}dt^2 + e^{2\alpha} (dr^2 + r^2d\theta^2) + e^{\gamma-\rho}r^2\sin^2\theta (d\phi - \omega dt)^2 \quad (3)$$

where α , γ , ρ and ω are the gravitational potentials which depend on r and θ only. The Einstein's equations for the three potentials γ , ρ and ω have been solved by Komatsu *et.al.* using Green's function technique. The fourth potential α has been determined from other potentials. All the physical quantities may then be determined from these potentials [24].

Solution of the potentials, and hence the calculation of physical quantities, is numerically quite an involved process. There are several numerical codes in the community for this purpose. In the present paper, using the **rns** code, developed by Stergioulas *et. al.*, we have studied the properties of rotating quark star. The results are discussed below.

Let us first look at the constant Ω (angular velocity) sequences. In figure 2 we have plotted mass as a function of radius for different angular velocities starting from the static up to the keplerian limit. For comparison, the $M - R$ curves for both CCDM and bag model have been plotted in the same figure. From this figure one can see that, in the static limit, for the same mass the CCDM gives a much smaller radius compared to the bag model. For example, in the static case, for a star with mass $1.6M_\odot$, the radius of a star is about 11 Km for bag model compared to about 9.5 Km for the CCDM. However, this difference is much more pronounced for rotating stars especially as we move towards the keplerian limit. For a star moving with keplerian frequency, in fact, there is no overlap between the mass-radius plots for the two models. As we vary the energy density from $8 \times 10^{14} \text{ gms/cm}^3$ to $1.5 \times 10^{15} \text{ gms/cm}^3$ the CCDM results in a mass range of $2.1M_\odot - 2.5M_\odot$ and the radius varies from 14 Km to 15 Km. For the same variation of energy density the bag model results in a mass variation from $2.9M_\odot$ to $3.2M_\odot$. The radius varies from 16.5 Km to 17.8 Km for such stars. However these results are better explained in figure 3 as discussed below.

In figure 3 we have plotted the mass as a function of central energy density. For $\epsilon_c = 1.2 \times 10^{15} \text{ gms/cm}^3$ the mass of a static star is about $1.3M_\odot$ in CCDM. For the same central energy density the bag model results in a star of mass $2M_\odot$. So there is a huge difference between the two models even in the static case. Let us now look at the other extreme limit. When the star is rotating with keplerian frequency a central density of $1.2 \times 10^{15} \text{ gms/cm}^3$ results in a star of mass $3.1M_\odot$ in the bag model and $2.2M_\odot$ in the CCDM.

The difference of the results obtained from the two models, as discussed above, can be ascribed to the difference in the EOSs of the two models. The softer EOS of CCDM allows a star to have smaller size compared to that in the bag model for the same mass.

Apart from the mass-radius relationship, one of the ways to look at the validity of an EOS is to look at the QPOs or the ISCO frequencies. For conventional rotating neutron stars the ISCO lies inside the star. However, this is not true for a rotating quark star. The ISCO frequencies are observable quantities and hence one can put a constraint

on the EOS from these results. We have studied the ISCO frequencies for both the models for different rotational frequencies. In figure 4 the QPO frequencies (Ω_+) have been plotted as a function of mass of the star, rotating with keplerian angular velocity, for the CCDM as well as the bag model. From figure 4 we can see that for both the models the ISCO frequency increases with mass. The ISCO frequencies obtained from the CCDM are found to be somewhat higher compared to the bag model for the same range of ϵ_c as mentioned earlier. In the case of CCDM the range of ISCO frequency is $1263Hz$ to $1490Hz$ where as for the bag model it is $1101Hz$ to $1351Hz$. It should be noted that for all the cases mentioned here, ISCO lies above the stellar surface. Furthermore, especially for the CCDM, reducing the rotational frequency of the star results in the vanishing of the gap between the ISCO and the stellar surface.

Rossi X-ray Timing Explorer (RXTE) has observed kHz QPOs in around 20 LMXBs, mostly showing double peaks. The high frequency peak, which corresponds to the the ISCO frequency lies in the range 500 - 1200 Hz [25]. Our results are comparable to the higher end of observed ranges. We would also like to mention here that the presence of crust for a star in CCDM causes the gap to vanish even for keplerian rotational frequency.

In figure 5 we have plotted the ISCO frequency as a function of the rotational frequency. As in figure 4, the rotational frequency is the keplerian frequency. It can be seen that for both the models the ISCO frequency increases with rotational frequency. Furthermore, star in bag model has lower Ω_+ compared to that in CCDM for the same value of Ω .

IV. SUMMARY AND DISCUSSION

We have studied the rotating compact stars within the framework of CCDM. This is the first time that CCDM has been employed towards the study of the rotating stars. The results have been compared with the bag model for same values of bag pressure and strong coupling. We have found that the results obtained from the CCDM is very different compared to those obtained in the bag model. The size of a star obtained in the bag model is much more compared to that in the CCDM for the same mass. Furthermore, the difference gets much more pronounced as one moves towards the keplerian limit. We have also studied the ISCO frequencies for these two models. For both the models Ω_+ increases with M. The Ω_+ is higher in CCDM compared to that in the bag model. In our model, only the QPOs having frequency higher than 1260 Hz can be a strange star.

There are several issues that remains to be addressed so far as the existence of the strange stars is concerned. Though it is true that the quark models can be constrained using the observed ISCO frequencies, while constructing the quark matter EOS, one should also try to incorporate the essential QCD symmetries into the model. This puts a further constraint on the quark matter EOS as it induces a qualitative difference in the EOS. For example, the bag model EOS can be easily put into the form $P = a(\rho - \rho_0)c^2/3$ [12] where a is a positive number. In contrast, the best possible fit for the CCDM model EOS is given by the polynomial form $P = a_0(\rho - \rho_0) + a_1(\rho - \rho_0)^{3/2}$. The coefficients are $a_0 = 2.7983 \times 10^{20}$ and $a_1 = 1.2245 \times 10^{12}$ with $\rho_0 \approx 5.7 \times 10^{14} \text{gms/cm}^3$.

Moreover, bag model EOS being stiffer, which resulted in a higher mass for the static star, people were in search of a softer model to yield a lower value of the star mass. It now seems that a stiffer EOS is preferable to reproduce the observed QPO frequencies. One should make a further survey of the models at this stage and look for better EOSs which can reproduce both the star mass and the QPO frequency satisfactorily.

Acknowledgements AB would like to thank University Grants Commission for partial support through the grant PSW-083/03-04.

[1] E. Witten, Phys. Rev. **D30**, 272 (1984).

- [2] E. Farhi and R. L. Jaffe, Phys. Rev. **D30**, 2379 (1984); **D32**, 2452 (1985); C. Alcock and et. al. Astrophys. J. **310**, 261 (1986); P. Haensel and et. al., Astron. & Astrophys., **160**, 121 (1986).
- [3] J. C. Collins and M. J. Perry, Phys. Rev. Lett. **34**, 1353 (1975); B. A. Freedman and L. D. McLerran, Phys. Rev. **D17**, 1109 (1978); B. D. Serot and H. Uechi, Ann. of Phys. **179**, 272 (1987).
- [4] S. K. Ghosh, S. C. Phatak and P. K. Sahu, Nucl. Phys. **A596**, 670 (1996).
- [5] N. K. Glendenning, S. Pei and F. Weber, Phys. Rev. Lett. **79**, 1603 (1997).
- [6] N. K. Spyrou and N. Stergioulas, Astron. & Astrophys. **395**, 151 (2002).
- [7] A. Bhattacharyya, S. K. Ghosh, M. Hanauske and S. Raha, Phys. Rev. **C71**, 048801 (2005).
- [8] I. N. Mishustin, M. Hanauske, A. Bhattacharyya, L. M. Satarov, H. Stoecker and W. Greiner, Phys. Lett. **B552**, 1 (2003).
- [9] K. Schertler, C. Greiner, J. Schaffner-Bielich and M. Thoma, Nucl. Phys. **A677**, 463 (2000).
- [10] I. Bombaci, Phys. Rev. **C55**, 1587 (1997); K. S. Cheng, Z. G. Dai, D. M. Wei and T. Lu, Science **280**, 407 (1998); Z. G. Dai and T. Lu, Phys. Rev. Lett. **81**, 4301 (1998).
- [11] E. Gourgoulhon, P. haensel, R. Livine, E. Paluch, S. Bonazzola and J. A. Marck, Astron. & Astrophys. **349**, 851 (1999).
- [12] N. Sterigioulas, W. Kluźniak and T. Bulik, Astron. & Astrophys. **352**, L116 (1999).
- [13] J. L Zdunik, P. Haensel, Gondek-Rosińska and E. Gourgoulhon, Astron. & Astrophys. **356**, 612 (2000).
- [14] F. Limousin, D. Gondek-Rosinska and E. Gourgoulhon, Phys. Rev. **D71**, 064012 (2005)
- [15] S. Sahu and S. C. Phatak, Mod. Phys. Lett. **A7**, 709 (1992).
- [16] S. C. Phatak, Phys. Rev. **44C**, 875 (1991).
- [17] S. K. Ghosh and S. C. Phatak, J. Phys. **G18**, 755 (1992); Phys. Rev. **C52**, 2195 (1995).
- [18] S. K. Ghosh and S. C. Phatak, Phys. Rev. **C58**, 1714 (1998).
- [19] S. K. Ghosh, S. C. Phatak and P. K. Sahu, Z. Phys. **A352**, 457 (1995).
- [20] S. K. Ghosh and P. K. Sahu, Int. J. Mod. Phys. **E2**, 575 (1993).
- [21] S. Theberg, A. W. Thomas and G. A. Miller, Phys. Rev. D **22**, 2838 (1980).
- [22] A. Chodos and C. B. Thorn, Phys. Rev. D **12**, 2733 (1975).
- [23] H. Komatsu, Y. Eriguchi and I. Hachisu, Mon. Not. R. Astr. Soc. **237**, 355 (1989).
- [24] G. B. Cook, S. L. Shapiro and S. A. Teukolsky, Ap. Jr. **424**, 823 (1994).
- [25] M. van der Klis, in Proceedings of the Third William Fairbank Meeting, astro-ph/9812395.

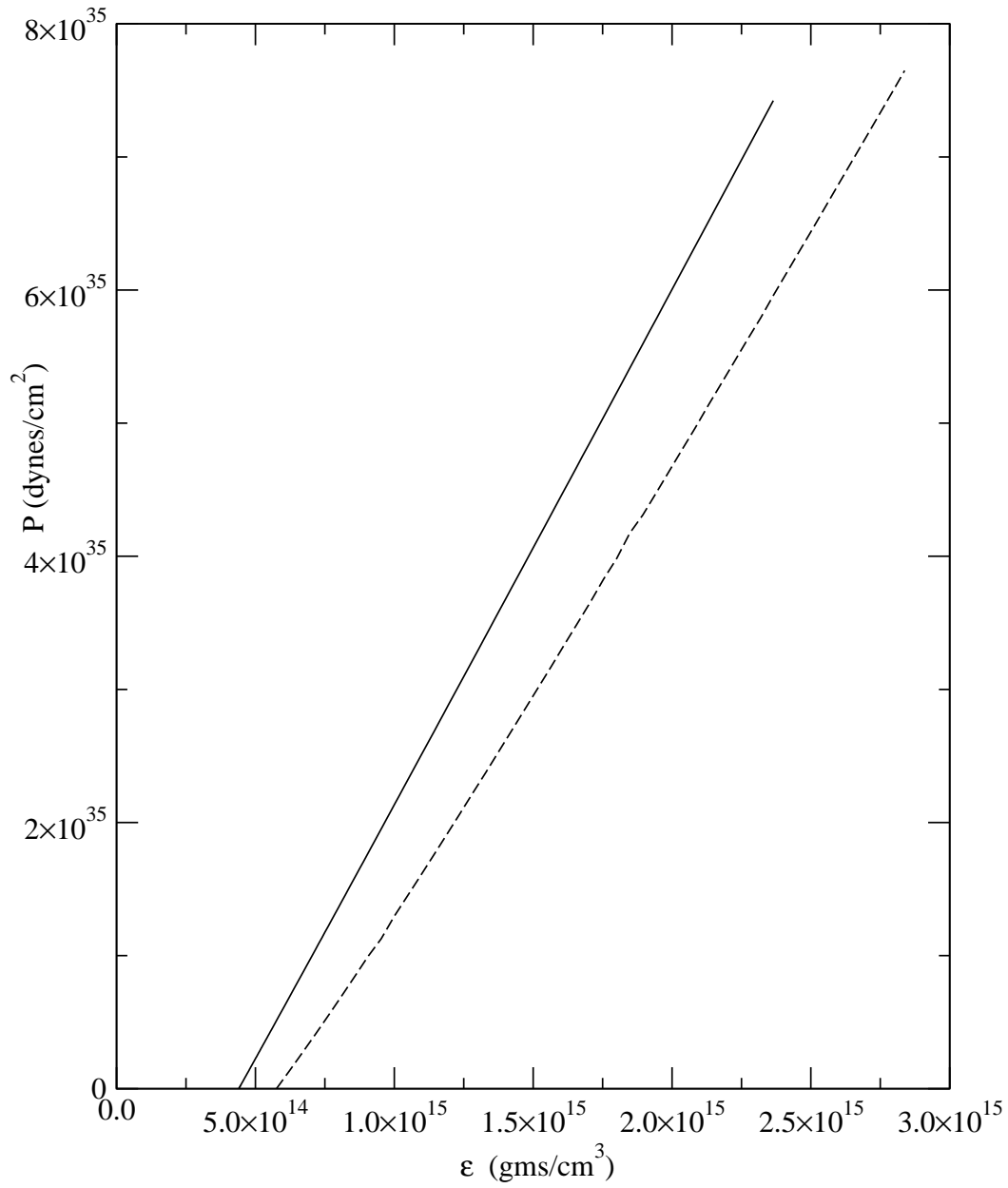


FIG. 1. EOSs obtained from the Bag model (continuous line) and CCDM (dashed line).

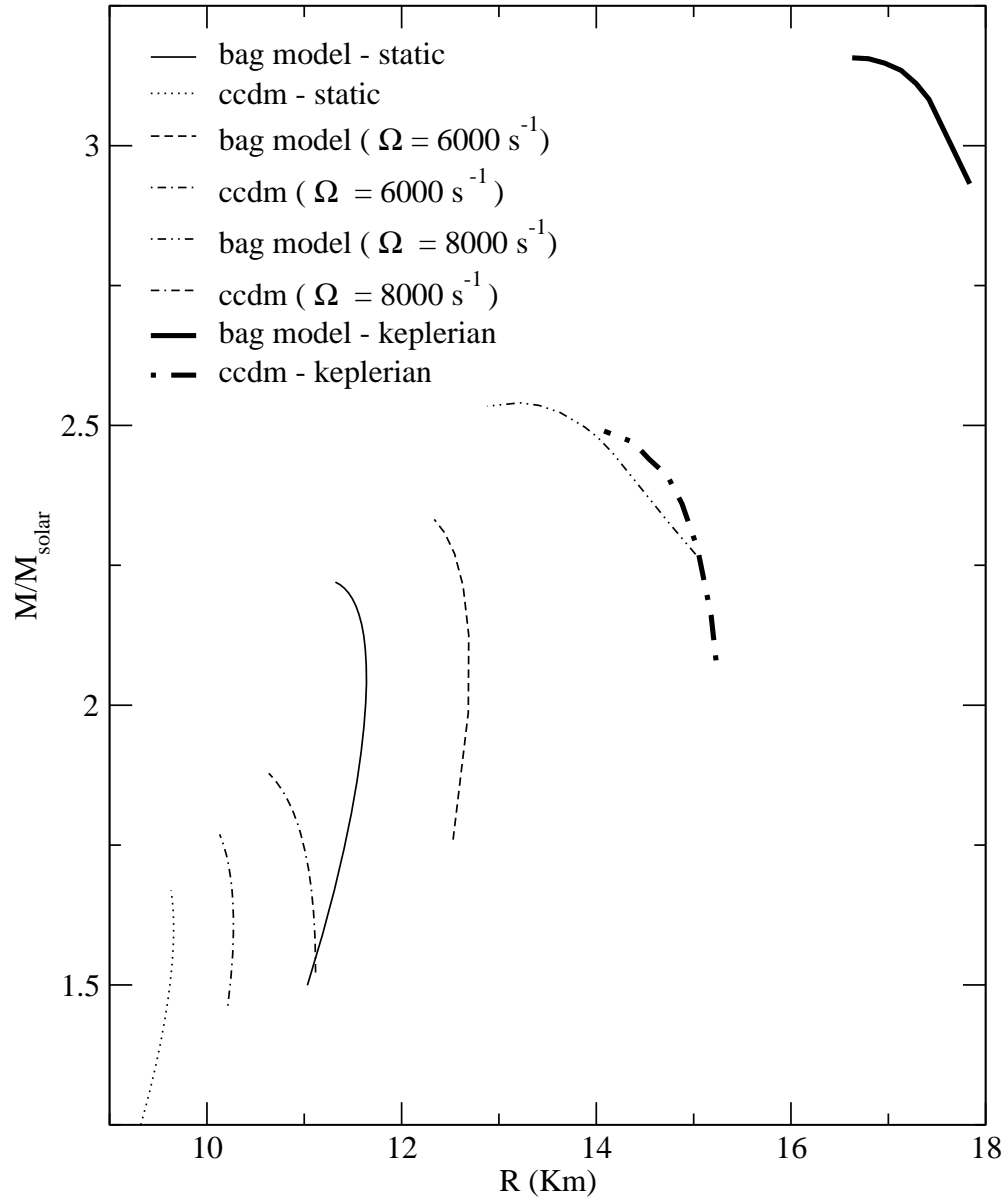


FIG. 2. Mass-Radius plots at constant Ω for different values of Ω .

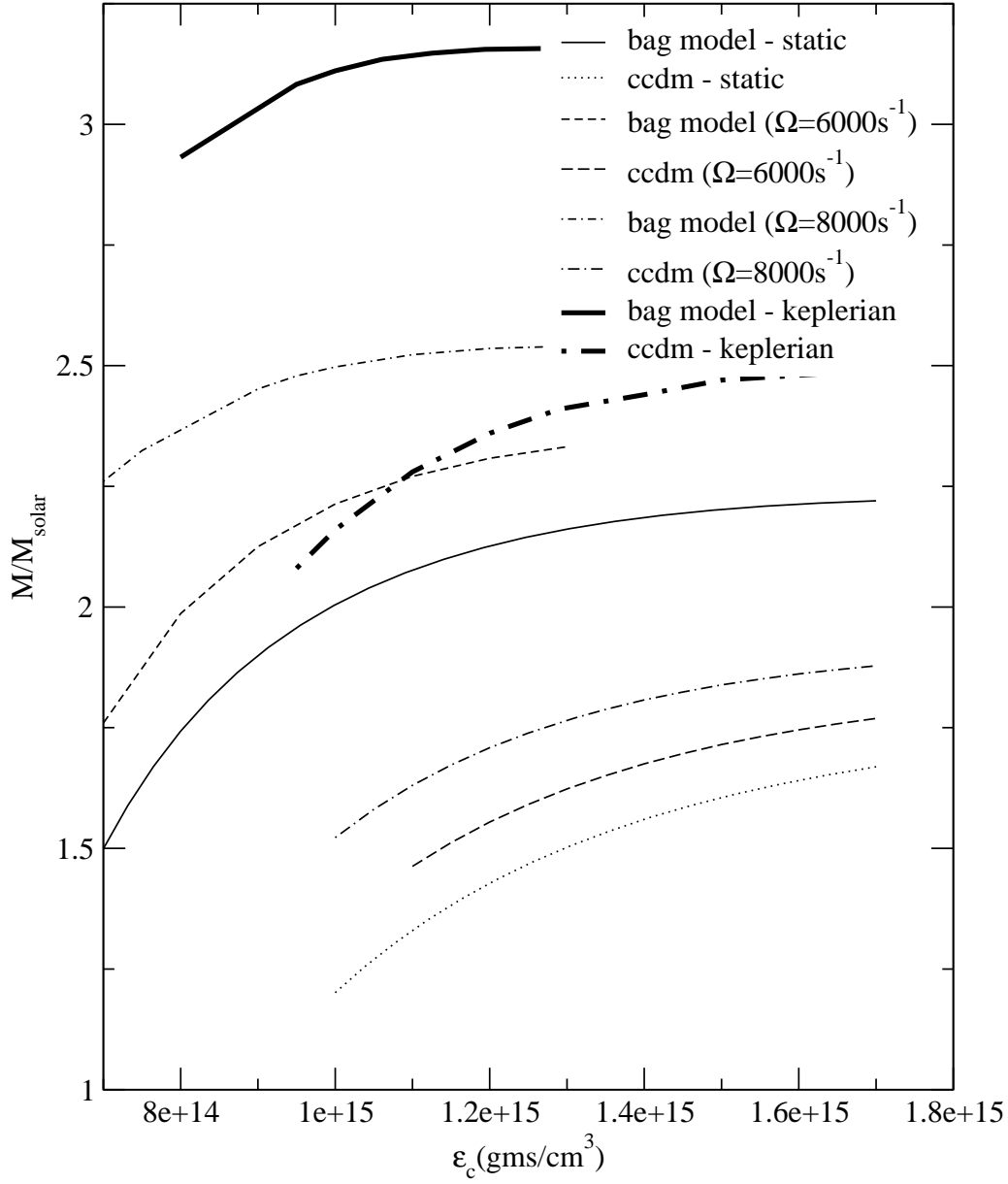


FIG. 3. Mass-Central density plots for constant Ω for different values of Ω .

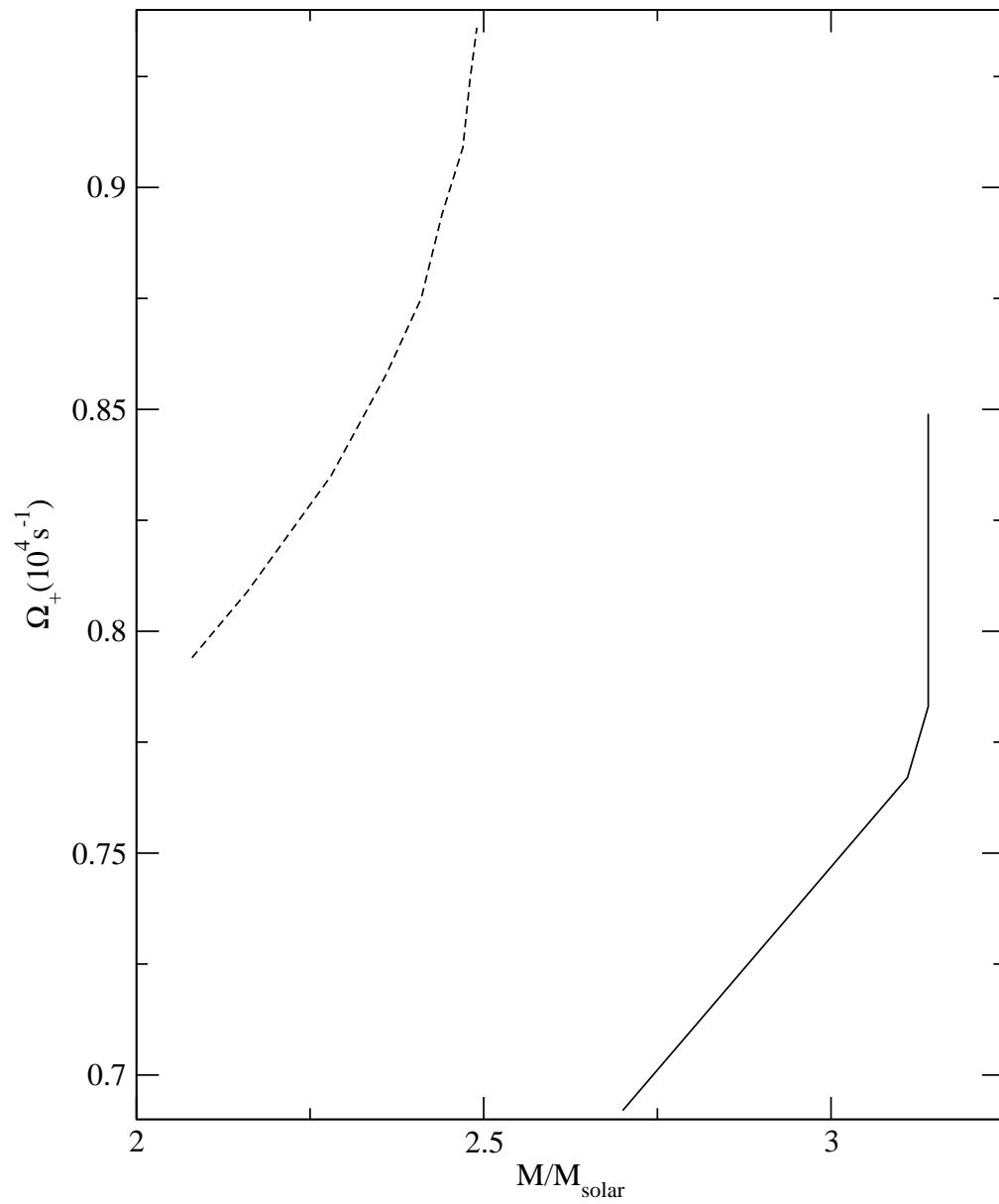


FIG. 4. Ω_+ as a function of mass for bag model (continuous line) and for ccdm (dashed line).

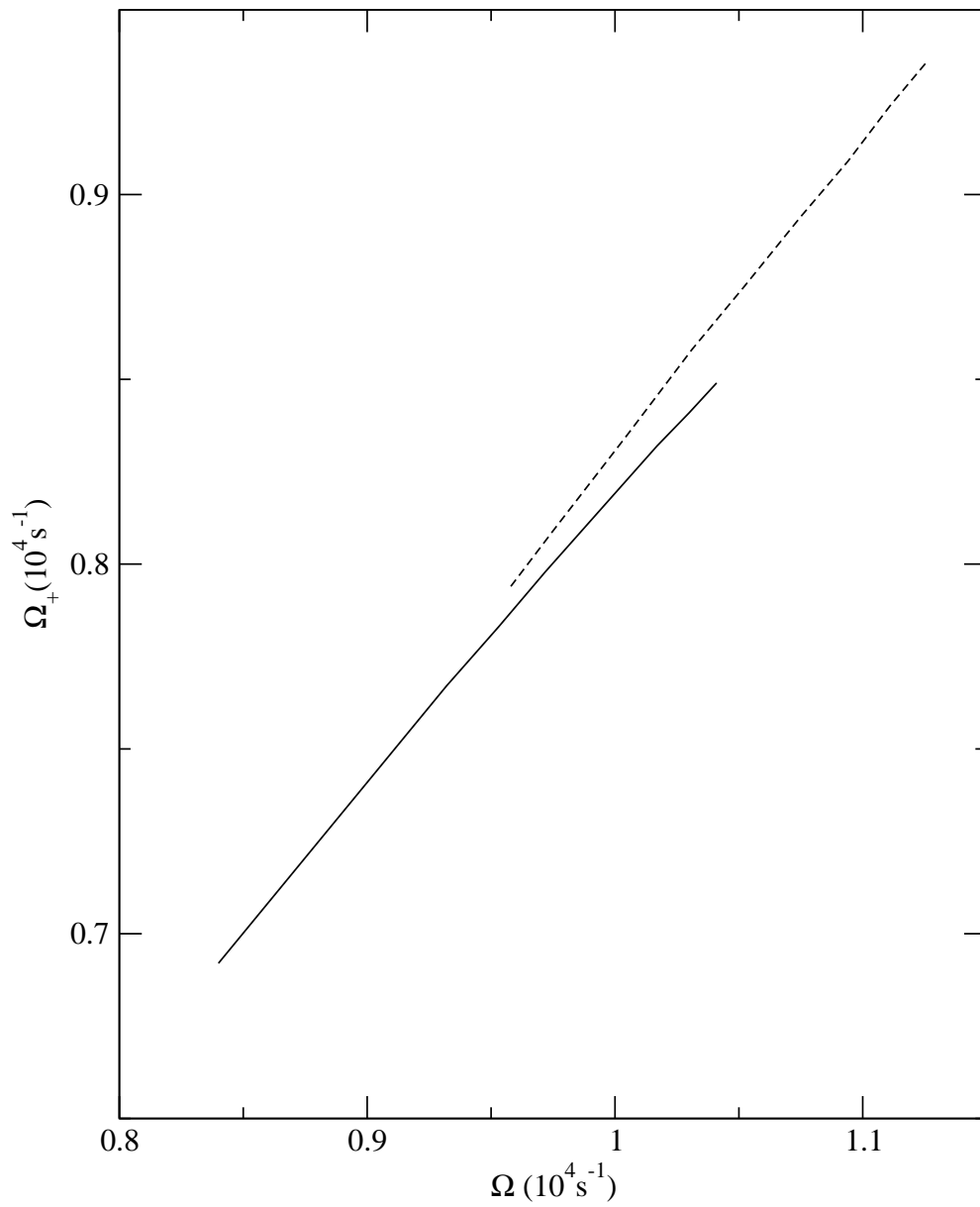


FIG. 5. Ω_+ as a function of Ω for bag model (continuous line) and for ccdm (dashed line).